

Chapter 8

Billiards

THE DYNAMICS that we have the best intuitive grasp on, and find easiest to grapple with both numerically and conceptually, is the dynamics of billiards. For billiards, discrete time is altogether natural; a particle moving through a billiard suffers a sequence of instantaneous kicks, and executes simple motion in between, so there is no need to contrive a Poincaré section. We have already used this system in sect. 1.3 as the intuitively most accessible example of chaos. Here we define billiard dynamics more precisely, anticipating the applications to come.

8.1 Billiard dynamics

A billiard is defined by a connected region $Q \subset \mathbb{R}^D$, with boundary $\partial Q \subset \mathbb{R}^{D-1}$ separating Q from its complement $\mathbb{R}^D \setminus Q$. The region Q can consist of one compact, finite volume component (in which case the billiard phase space is bounded, as for the stadium billiard of figure 8.1), or can be infinite in extent, with its complement $\mathbb{R}^D \setminus Q$ consisting of one or several finite or infinite volume components (in which case the phase space is open, as for the 3-disk pinball game in figure 1.1). In what follows we shall most often restrict our attention to *planar billiards*.

A point particle of mass m and momentum $p_n = mv_n$ moves freely within the billiard, along a straight line, until it encounters the boundary. There it reflects specularly (*specular* = mirrorlike), with no change in the tangential component of momentum, and instantaneous reversal of the momentum component normal to the boundary,

$$p' = p - 2(p \cdot \hat{n})\hat{n}, \tag{8.1}$$

with \hat{n} the unit vector normal to the boundary ∂Q at the collision point. The angle of incidence equals the angle of reflection, as illustrated in figure 8.2. A billiard is

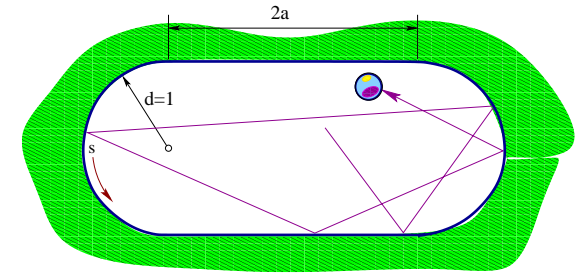


Figure 8.1: The stadium billiard is a 2-dimensional domain bounded by two semi-circles of radius $d = 1$ connected by two straight walls of length $2a$. At the points where the straight walls meet the semi-circles, the curvature of the border changes discontinuously; these are the only singular points of the flow. The length a is the only parameter.

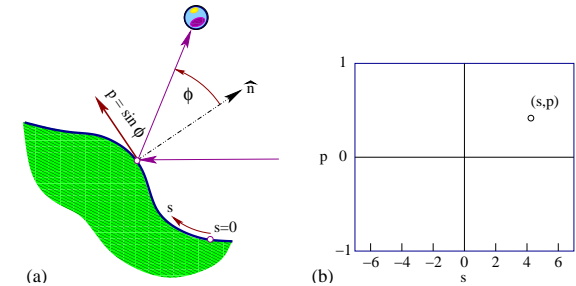


Figure 8.2: (a) A planar billiard trajectory is fixed by specifying the perimeter length parametrized by s and the outgoing trajectory angle ϕ , both measured counterclockwise with respect to the outward normal \hat{n} . (b) The Birkhoff phase-space coordinate pair (s, p) fully specifies the trajectory, where $p = |p| \sin \phi$ is the momentum component tangential to the boundary. As the pinball kinetic energy is conserved in elastic scattering, the pinball mass and the magnitude of the pinball momentum are customarily set to $m = |p| = 1$.

a Hamiltonian system with a $2D$ -dimensional phase space $x = (q, p)$ and potential $V(q) = 0$ for $q \in Q$, $V(q) = \infty$ for $q \in \partial Q$.

remark 2.1

A billiard flow has a natural Poincaré section defined by Birkhoff coordinates s_n , the arc length position of the n th bounce measured along the billiard boundary, and $p_n = |p| \sin \phi_n$, the momentum component parallel to the boundary, where ϕ_n is the angle between the outgoing trajectory and the normal to the boundary. We measure both the arc length s , and the parallel momentum p counterclockwise relative to the outward normal (see figure 8.2 as well as figure 3.9 (a)). In $D = 2$, the Poincaré section is a cylinder (topologically an annulus), figure 8.3, where the parallel momentum p ranges for $-|p|$ to $|p|$, and the s coordinate is cyclic along each connected component of ∂Q . The volume in the full phase space is preserved by the Liouville theorem (7.39). The Birkhoff coordinates $x = (s, p) \in \mathcal{P}$, are the natural choice, because with them the Poincaré return map preserves the phase-space volume of the (s, p) parameterized Poincaré section (a perfectly good coordinate set (s, ϕ) does not do that).

exercise 8.6

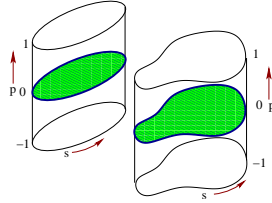
exercise 8.6 section 8.2

Without loss of generality we set $m = |v| = |p| = 1$. Poincaré section condition eliminates one dimension, and the energy conservation $|p| = 1$ eliminates another, so the Poincaré section return map P is $(2D - 2)$ -dimensional.

The dynamics is given by the Poincaré return map

$$P : (s_n, p_n) \mapsto (s_{n+1}, p_{n+1}) \tag{8.2}$$

Figure 8.3: In $D = 2$ the billiard Poincaré section is a cylinder, with the parallel momentum p ranging over $p \in [-1, 1]$, and with the s coordinate is cyclic along each connected component of ∂Q . The rectangle figure 8.2(b) is such cylinder unfolded, with periodic boundary conditions glueing together the left and the right edge of the rectangle.



from the n th collision to the $(n + 1)$ st collision. The discrete time dynamics map P is equivalent to the Hamiltonian flow (7.1) in the sense that both describe the same full trajectory. Let t_n denote the instant of n th collision. Then the position of the pinball $\in Q$ at time $t_n + \tau \leq t_{n+1}$ is given by $2D - 2$ Poincaré section coordinates $(s_n, p_n) \in \mathcal{P}$ together with τ , the distance reached by the pinball along the n th section of its trajectory (as we have set the pinball speed to 1, the time of flight equals the distance traversed).

Example 8.1 3-disk game of pinball: In the case of bounces off a circular disk, the position coordinate $s = r\theta$ is given by angle $\theta \in [0, 2\pi]$. For example, for the 3-disk game of pinball of figure 1.6 and figure 3.9(a) we have two types of collisions: exercise 8.1

$$P_0 : \begin{cases} \phi' = -\phi + 2 \arcsin p \\ p' = -p + \frac{a}{R} \sin \phi' \end{cases} \quad \text{back-reflection} \quad (8.3)$$

$$P_1 : \begin{cases} \phi' = \phi - 2 \arcsin p + 2\pi/3 \\ p' = p - \frac{a}{R} \sin \phi' \end{cases} \quad \text{reflect to 3rd disk.} \quad (8.4)$$

Here a = radius of a disk, and R = center-to-center separation. Actually, as in this example we are computing intersections of circles and straight lines, nothing more than high-school geometry is required. There is no need to compute arcsin - one only needs to compute one square root per each reflection, and the simulations can be very fast. exercise 8.2

Trajectory of the pinball in the 3-disk billiard is generated by a series of P_0 's and P_1 's. At each step one has to check whether the trajectory intersects the desired disk (and no disk in-between). With minor modifications, the above formulas are valid for any smooth billiard as long as we replace a by the local curvature of the boundary at the point of collision.

8.2 Stability of billiards

We turn next to the question of local stability of discrete time billiard systems. Infinitesimal equations of variations (4.2) do not apply, but the multiplicative structure (4.39) of the finite-time Jacobian matrices does. As they are more physical than most maps studied by dynamicists, let us work out the billiard stability in some detail.

On the face of it, a plane billiard phase space is 4-dimensional. However, one dimension can be eliminated by energy conservation, and the other by the fact that the magnitude of the speed is constant. We shall now show how going to a local frame of motion leads to a $[2 \times 2]$ Jacobian matrix.

Consider a 2-dimensional billiard with phase-space coordinates $x = (q_1, q_2, p_1, p_2)$. Let t_n be the instant of the n th collision of the pinball with the billiard boundary, and $t_n^\pm = t_n \pm \epsilon$, ϵ positive and infinitesimal. With the mass and the speed equal to 1, the momentum direction can be specified by angle θ : $x = (q_1, q_2, \sin \theta, \cos \theta)$. Now parametrize the 2 - dimensional neighborhood of a trajectory segment by $\delta x = (\delta z, \delta \theta)$, where

$$\delta x = \delta q_1 \cos \theta - \delta q_2 \sin \theta, \quad (8.5)$$

$\delta \theta$ is the variation in the direction of the pinball motion. Due to energy conservation, there is no need to keep track of $\delta q_{||}$, variation along the flow, as that remains constant. $(\delta q_1, \delta q_2)$ is the coordinate variation transverse to the k th segment of the flow. From the Hamilton's equations of motion for a free particle, $dq_i/dt = p_i$, $dp_i/dt = 0$, we obtain the equations of motion (4.1) for the linearized neighborhood

$$\frac{d}{dt} \delta \theta = 0, \quad \frac{d}{dt} \delta z = \delta \theta. \quad (8.6)$$

Let $\delta \theta_n = \delta \theta(t_n^+)$ and $\delta z_n = \delta z(t_n^+)$ be the local coordinates immediately after the n th collision, and $\delta \theta_n^- = \delta \theta(t_n^-)$, $\delta z_n^- = \delta z(t_n^-)$ immediately before. Integrating the free flight from t_{n-1}^+ to t_n^- we obtain

$$\begin{aligned} \delta z_n^- &= \delta z_{n-1} + \tau_n \delta \theta_{n-1}, & \tau_n &= t_n - t_{n-1} \\ \delta \theta_n^- &= \delta \theta_{n-1}, \end{aligned} \quad (8.7)$$

and the Jacobian matrix (4.38) for the n th free flight segment is

$$M_T(x_n) = \begin{pmatrix} 1 & \tau_n \\ 0 & 1 \end{pmatrix}. \quad (8.8)$$

At incidence angle ϕ_n (the angle between the outgoing particle and the outgoing normal to the billiard edge), the incoming transverse variation δz_n^- projects onto an arc on the billiard boundary of length $\delta z_n^- / \cos \phi_n$. The corresponding incidence angle variation $\delta \phi_n = \delta z_n^- / \rho_n \cos \phi_n$, ρ_n = local radius of curvature, increases the angular spread to

$$\begin{aligned} \delta z_n &= -\delta z_n^- \\ \delta \theta_n &= -\delta \theta_n^- - \frac{2}{\rho_n \cos \phi_n} \delta z_n^-, \end{aligned} \quad (8.9)$$

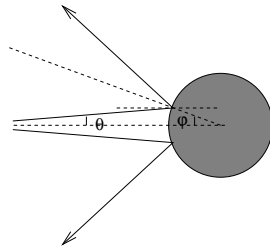


Figure 8.4: Defocusing of a beam of nearby trajectories at a billiard collision. (A. Wirzba)

so the Jacobian matrix associated with the reflection is

$$M_R(x_n) = - \begin{pmatrix} 1 & 0 \\ r_n & 1 \end{pmatrix}, \quad r_n = \frac{2}{\rho_n \cos \phi_n}. \quad (8.10)$$

The full Jacobian matrix for n_p consecutive bounces describes a beam of trajectories defocused by M_T along the free flight (the τ_n terms below) and defocused/refocused at reflections by M_R (the r_n terms below)

exercise 8.4

$$M_p = (-1)^{n_p} \prod_{n=1}^{n_p} \begin{pmatrix} 1 & \tau_n \\ 0 & 1 \end{pmatrix} \begin{pmatrix} 1 & 0 \\ r_n & 1 \end{pmatrix}, \quad (8.11)$$

where τ_n is the flight time of the k th free-flight segment of the orbit, $r_n = 2/\rho_n \cos \phi_n$ is the defocusing due to the k th reflection, and ρ_n is the radius of curvature of the billiard boundary at the n th scattering point (for our 3-disk game of pinball, $\rho = 1$). As the billiard dynamics is phase-space volume preserving, $\det M = 1$, and the eigenvalues are given by (7.30).

This is an example of the Jacobian matrix chain rule (4.47) for discrete time systems (the Hénon map stability (4.48) is another example). Stability of every flight segment or reflection taken alone is a shear with two unit eigenvalues,

$$\det M_T = \det \begin{pmatrix} 1 & \tau_n \\ 0 & 1 \end{pmatrix}, \quad \det M_R = \det \begin{pmatrix} 1 & 0 \\ r_n & 1 \end{pmatrix}, \quad (8.12)$$

but acting in concert in the interwoven sequence (8.11) they can lead to a hyperbolic deformation of the infinitesimal neighborhood of a billiard trajectory.

exercise 13.7

As a concrete application, consider the 3-disk pinball system of sect. 1.3. Analytic expressions for the lengths and eigenvalues of $\bar{0}$, $\bar{1}$ and $\bar{10}$ cycles follow from elementary geometrical considerations. Longer cycles require numerical evaluation by methods such as those described in chapter 13.

exercise 13.8
exercise 8.3
chapter 13

Résumé

A particular natural application of the Poincaré section method is the reduction of a billiard flow to a boundary-to-boundary return map.

Commentary

Remark 8.1 Billiards. The 3-disk game of pinball is to chaotic dynamics what a pendulum is to integrable systems; the simplest physical example that captures the essence of chaos. Another contender for the title of the ‘harmonic oscillator of chaos’ is the baker’s map which is used as the red thread through Ott’s introduction to chaotic dynamics [1.11]. The baker’s map is the simplest reversible dynamical system which is hyperbolic and has positive entropy. We will not have much use for the baker’s map here, as due to its piecewise linearity it is so nongeneric that it misses all of the subtleties of cycle expansions curvature corrections that will be central to this treatise.

chapter 20

That the 3-disk game of pinball is a quintessential example of deterministic chaos appears to have been first noted by B. Eckhardt [8.1]. The model was studied in depth classically, semiclassically and quantum mechanically by P. Gaspard and S.A. Rice [8.3], and used by P. Cvitanović and B. Eckhardt [8.4] to demonstrate applicability of cycle expansions to quantum mechanical problems. It has been used to study the higher order \hbar corrections to the Gutzwiller quantization by P. Gaspard and D. Alonso Ramirez [8.5], construct semiclassical evolution operators and entire spectral determinants by P. Cvitanović and G. Vattay [8.6], and incorporate the diffraction effects into the periodic orbit theory by G. Vattay, A. Wirzba and P.E. Rosenqvist [8.7]. Gaspard’s monograph [1.8], which we warmly recommend, utilizes the 3-disk system in much more depth than will be attained here. For further links check ChaosBook.org.

A pinball game does miss a number of important aspects of chaotic dynamics: generic bifurcations in smooth flows, the interplay between regions of stability and regions of chaos, intermittency phenomena, and the renormalization theory of the ‘border of order’ between these regions. To study these we shall have to face up to much harder challenge, dynamics of smooth flows.

Nevertheless, pinball scattering is relevant to smooth potentials. The game of pinball may be thought of as the infinite potential wall limit of a smooth potential, and pinball symbolic dynamics can serve as a *covering* symbolic dynamics in smooth potentials. One may start with the infinite wall limit and adiabatically relax an unstable cycle onto the corresponding one for the potential under investigation. If things go well, the cycle will remain unstable and isolated, no new orbits (unaccounted for by the pinball symbolic dynamics) will be born, and the lost orbits will be accounted for by a set of pruning rules. The validity of this adiabatic approach has to be checked carefully in each application, as things can easily go wrong; for example, near a bifurcation the same naive symbol string assignments can refer to a whole island of distinct periodic orbits.

section 29.1

Remark 8.2 Stability analysis. The chapter 1 of Gaspard monograph [1.8] is recommended reading if you are interested in Hamiltonian flows, and billiards in particular. A. Wirzba has generalized the stability analysis of sect. 8.2 to scattering off 3-dimensional spheres (follow the links in ChaosBook.org/extras). A clear discussion of linear stability for the general d -dimensional case is given in Gaspard [1.8], sect. 1.4.

Exercises

- 8.1. **A pinball simulator.** Implement the disk \rightarrow disk maps to compute a trajectory of a pinball for a given starting point, and a given $R:a$ = (center-to-center distance):(disk radius) ratio for a 3-disk system. As this requires only computation of intersections of lines and circles together with specular reflections, implementation should be within reach of a high-school student. Please start working on this program now; it will be continually expanded in chapters to come, incorporating the Jacobian calculations, Newton root-finding, and so on. Fast code will use elementary geometry (only one $\sqrt{\dots}$ per iteration, rest are multiplications) and eschew trigonometric functions. Provide a graphic display of the trajectories and of the Poincaré section iterates. To be able to compare with the numerical results of coming chapters, work with $R:a = 6$ and/or 2.5 values. Draw the correct versions of figure 1.9 or figure 12.3 for $R:a = 2.5$ and/or 6.
- 8.2. **Trapped orbits.** Shoot 100,000 trajectories from one of the disks, and trace out the strips of figure 1.9 for various $R:a$ by color coding the initial points in the Poincaré section by the number of bounces preceding their escape. Try also $R:a = 6:1$, though that might be too thin and require some magnification. The initial conditions can be randomly chosen, but need not - actually a clearer picture is obtained by systematic scan through regions of interest.
- 8.3. **Pinball stability.** Add to your exercise 8.1 pinball simulator a routine that computes the $[2 \times 2]$ Jacobian matrix. To be able to compare with the numerical results of coming chapters, work with $R:a = 6$ and/or 2.5 values.
- 8.4. **Stadium billiard.** Consider the *Bunimovich stadium* [8.9, 8.10] defined in figure 8.1. The Jacobian matrix associated with the reflection is given by (8.10).

Here we take $\rho_k = -1$ for the semicircle sections of the boundary, and $\cos \phi_k$ remains constant for all bounces in a rotation sequence. The time of flight between two semicircle bounces is $\tau_k = 2 \cos \phi_k$. The Jacobian matrix of one semicircle reflection followed by the flight to the next bounce is

$$\begin{aligned} \mathbf{J} &= (-1) \begin{pmatrix} 1 & 2 \cos \phi_k \\ 0 & 1 \end{pmatrix} \begin{pmatrix} 1 & 0 \\ -2/\cos \phi_k & 1 \end{pmatrix} \\ &= (-1) \begin{pmatrix} -3 & 2 \cos \phi_k \\ 2/\cos \phi_k & 1 \end{pmatrix}. \end{aligned}$$

A free flight must always be followed by $k = 1, 2, 3, \dots$ bounces along a semicircle, hence the natural symbolic dynamics for this problem is n -ary, with the corresponding Jacobian matrix given by shear (i.e. the eigenvalues remain equal to 1 throughout the whole rotation), and k bounces inside a circle lead to

$$\mathbf{J}^k = (-1)^k \begin{pmatrix} -2k - 1 & 2k \cos \phi \\ 2k/\cos \phi & 2k - 1 \end{pmatrix}. \quad (8.13)$$

The Jacobian matrix of a cycle p of length n_p is given by

$$\mathbf{J}_p = (-1)^{\sum n_k} \prod_{k=1}^{n_p} \begin{pmatrix} 1 & \tau_k \\ 0 & 1 \end{pmatrix} \begin{pmatrix} 1 & 0 \\ n_k r_k & 1 \end{pmatrix}. \quad (8.14)$$

Adopt your pinball simulator to the stadium billiard.

- 8.5. **A test of your pinball simulator.** Test your exercise 8.3 pinball simulator by computing numerically cycle stabilities by tracking distances to nearby orbits. Compare your result with the exact analytic formulas of exercise 13.7 and 13.8.
- 8.6. **Birkhoff coordinates.** Prove that the Birkhoff coordinates are phase-space volume preserving.

References

- [8.1] B. Eckhardt, *Fractal properties of scattering singularities*, *J. Phys. A* **20**, 5971 (1987).
- [8.2] G.D. Birkhoff, *Acta Math.* **50**, 359 (1927), reprinted in ref. [1.24].

- [8.3] P. Gaspard and S.A. Rice, *J. Chem. Phys.* **90**, 2225 (1989); **90**, 2242 (1989); **90**, 2255 (1989).
- [8.4] P. Cvitanović and B. Eckhardt, "Periodic-orbit quantization of chaotic system," *Phys. Rev. Lett.* **63**, 823 (1989).
- [8.5] P. Gaspard and D. Alonso Ramirez, *Phys. Rev. A* **45**, 8383 (1992).
- [8.6] P. Cvitanović and G. Vattay, *Phys. Rev. Lett.* **71**, 4138 (1993).
- [8.7] G. Vattay, A. Wirzba and P.E. Rosenqvist, *Phys. Rev. Lett.* **73**, 2304 (1994).
- [8.8] Ya.G. Sinai, *Usp. Mat. Nauk* **25**, 141 (1970).
- [8.9] L.A. Bunimovich, *Funct. Anal. Appl.* **8**, 254 (1974).
- [8.10] L.A. Bunimovich, *Comm. Math. Phys.* **65**, 295 (1979).
- [8.11] L. Bunimovich and Ya.G. Sinai, *Markov Partition for Dispersed Billiard*, *Comm. Math. Phys.* **78**, 247 (1980); **78**, 479 (1980); *Erratum, ibid.* **107**, 357 (1986).
- [8.12] R. Bridges, "The spin of a bouncing 'superball,'" *Phys. Educ.* **26**, 350 (1991); www.iop.org/EJ/abstract/0031-9120/26/6/003
- [8.13] H. Lamba, "Chaotic, regular and unbounded behaviour in the elastic impact oscillator;" [arXiv:chao-dyn/9310004](https://arxiv.org/abs/9310004).
- [8.14] S.W. Shaw and P.J. Holmes, *Phys. Rev. Lett.* **51**, 623 (1983).
- [8.15] C.R. de Oliveira and P.S. Goncalves, "Bifurcations and chaos for the quasiperiodic bouncing ball," *Phys. Rev. E* **56**, 4868 (1997).
- [8.16] E. Cataldo and R. Sampaio, "A Brief Review and a New Treatment for Rigid Bodies Collision Models," *J. Braz. Soc. Mech. Sci.* **23** (2001).
- [8.17] J. M. T. Thompson and R. Ghaffari. *Phys. Lett. A* **91**, 5 (1982).
- [8.18] J.M.T. Thompson, A.R. Bokaian and R. Ghaffari. *J. Energy Resources Technology (Trans ASME)*, **106**, 191-198 (1984).
- [8.19] E. Fermi. *Phys. Rev.* **75**, 1169 (1949).
- [8.20] J. P. Cleveland, B. Anczykowski, i A. E. Schmid, and V. B. Elings. *Appl. Phys. Lett.* **72**, 2613 (1998).
- [8.21] G. A. Tomlinson, *Philos. Mag* **7**, 905 (1929).
- [8.22] T. Gyalog and H. Thomas, *Z. Phys. Lett. B* **104**, 669 (1997).
- [8.23] J. Berg and G. A. D. Briggs. *Phys. Rev. B* **55**, 14899 (1997).
- [8.24] J. Guckenheimer, P. J. Holmes. *J. Sound Vib.* **84**, 173 (1982).
- [8.25] J. M. Luck, Anita Mehta *Phys. Rev. E* **48**, 3988 (1993).

- [8.26] A. Valance, D. Bideau. *Phys. Rev. E* **57**, 1886 (1998).
- [8.27] S.M. Hammel, J.A. Yorke, and C. Grebogi. *J. Complexity* **3**, 136 (1987).
- [8.28] L. Mañyaś, R. Klages. *Physica D* **187**, 165 (2004).